Hindawi
Complexity
Volume 2022, Article ID 8531858, 11 pages
https://doi.org/10.1155/2022/8531858

Research Article

ABC Fractional Derivative for the Alcohol Drinking Model using Two-Scale Fractal Dimension

Qura Tul Ain,[1] T. Sathiyaraj,[2] Shazia Karim,[3] Muhammad Nadeem,[4] and Patrick Kandege Mwanakatwe[5]

[1]*Department of Mathematics, Guizhou University, Guiyang 550025, China*
[2]*Institute of Actuarial Science and Data Analytics, UCSI University, Cheers 56000, Malaysia*
[3]*Department of Basic Sciences, FSD Campus, UET Lahore, Lahore, Pakistan*
[4]*Faculty of Science, Yibin University, Yibin 644000, China*
[5]*Eastern Africa Statistical Training Center, Dar es Salaam, Tanzania*

Correspondence should be addressed to Patrick Kandege Mwanakatwe; patrick26573@yahoo.co.uk

Received 22 March 2022; Revised 4 May 2022; Accepted 13 May 2022; Published 6 June 2022

Academic Editor: C. Rajivganthi

Drinking kills a significant proportion of individuals every year, particularly in low-income communities. An impulsive differential equation system is used to explore the effectiveness of activated charcoal in detoxifying the body after methanol poisoning. Our impression of activated charcoal is shaped by the fractional dynamics of the problem, which leads to speedy and low-cost first aid. The adsorption capacity of activated charcoal is investigated using impulsive differential equations. The ABC fractional operator's findings paint a more realistic image of first aid in public and primary health centers, which can assist to reduce methanol poisoning deaths. Numerical simulations are provided using generalized Adams–Bashforth–Moulton method (GABMM).

1. Introduction

Drinking is responsible for around 3.3 million deaths per year, with the majority of these deaths occurring without primary therapy [1]. The lack of good health-care facilities is a primary cause of untreated mortality. It is critical because of its impact on backward social and economic classes. The mortality rate caused by methanol poisoning can be lowered by using activated charcoal. Activated charcoal's adsorption action ensures that it has healing and cleansing properties. The negatively charged porous structure of activated charcoal attracts positive molecules, accumulating toxins from the stomach and finally removing them from the body [2–4]. Fractional derivative models are used for precise modeling of those systems which require precise damping modeling. In recent years, different analytical and numerical approaches have been proposed in these areas, including their applications to new problems [5, 6]. Mathematical simulation of real life problems typically leads to fractional differential equations and other problems; in one or more variables, essential functions of mathematical physics, as well as their extensions and generalizations, are included. Furthermore, most physical fluid dynamics phenomena, quantum mechanics, electricity, ecological structures, and many other models are regulated by fractional-order PDEs within their scope of validity [7–9]. Modern advances in theoretical and applied science have primarily relied on understanding of the positive integer-order derivatives and integrals. The features of mathematical functions, ranging from gamma and beta functions through special functions, as well as integral differential operators with convolutional integrals and singularities, exists. The solution of many relevant problems leads to integral equations, which have little in common with the integral equation of Abel at first glance, and additional efforts are made for the development of tiles of analytical or computational methods to solve these equations due to this impression. However, their conversion to the form of the integral equation of Abel can also be convenient.

The growth of fractional calculus theory was slow in the beginning due to a lack of context in practical applications. Mandelbrot proposed the "fractal" idea first, pointing out that there are multiple fractal dimensions in nature as well as several challenges in science and technology and implying that there is a self-similar phenomenon. Fractional calculus theory and FDE theory have swiftly emerged as the dynamic foundation of fractal geometry and fractal dimension and have become a popular academic topic around the world. Fractional calculus is an excellent way to define physical memory and heredity. Fractional differential equations have increased in popularity as the response of the fractional-order system and eventually converge with the equations of the integer-order [10]. Many different types of physical systems use special functions, elliptic functions, and elliptic integrals. Their presence is well-known in the solution of nonlinear differential equations. These functions and integrals can be studied in [11–15]. Over the last few decades, fractional differential equations and fractional operators have emerged as reliable and well-organized mathematical tools for analyzing a wide range of scientific and engineering events [16, 17]. Unlike the differential equation with integer orders, the differential equation of fractional orders can display nonlocal relations with memory kernels in time and space.

Mathematical modeling of physical systems has many successful applications in engineering and sciences such as medical science, nanotechnology, biological processes, space sciences, and artificial intelligence [18–20]. Mathematical modeling is a wide field that draws the attention of scientists, engineers, and mathematicians to solve the many problems facing humankind [21–24]. We will use the Atangana–Baleanu fractional operator in Caputo sense to examine the fractional dynamics of given model. The reason for using Atangana–Baleanu fractional derivatives is its nonlocal properties. This operator can also capture complex behavior more effectively than other operators:

$$
\begin{aligned}
{}_0^{ABC}D_t^{\alpha}E_1^{\bullet} &= -k_1^{\bullet}E_1^{\bullet}M^{\bullet} + k_{-1}^{\bullet}C_1^{\bullet} + k_2^{\bullet}C_1^{\bullet} - k_5^{\bullet}E_1^{\bullet}I^{\bullet} + k_{-5}^{\bullet}C_3^{\bullet} + k_6^{\bullet}C_3^{\bullet},\\
{}_0^{ABC}D_t^{\alpha}M^{\bullet} &= -k_1^{\bullet}E_1^{\bullet}M^{\bullet} + k_{-1}^{\bullet}C_1^{\bullet},\\
{}_0^{ABC}D_t^{\alpha}C_1^{\bullet} &= k_1^{\bullet}E_1^{\bullet}M^{\bullet} - k_{-1}^{\bullet}C_1^{\bullet} - k_2^{\bullet}C_2^{\bullet},\\
{}_0^{ABC}D_t^{\alpha}P_1^{\bullet} &= k_2^{\bullet}C_1^{\bullet} - k_3^{\bullet}P_1^{\bullet}E_2^{\bullet} + k_{-3}^{\bullet}C_2^{\bullet},\\
{}_0^{ABC}D_t^{\alpha}E_2^{\bullet} &= -k_3^{\bullet}P_1^{\bullet}E_2^{\bullet} + k_{-3}^{\bullet}C_2^{\bullet} + k_4^{\bullet}C_2^{\bullet},\\
{}_0^{ABC}D_t^{\alpha}C_2^{\bullet} &= k_3^{\bullet}P_1^{\bullet}E_2^{\bullet} - k_{-3}^{\bullet}C_2^{\bullet} - k_4^{\bullet}C_2^{\bullet},\\
{}_0^{ABC}D_t^{\alpha}P_2^{\bullet} &= k_4^{\bullet}C_2^{\bullet},\\
{}_0^{ABC}D_t^{\alpha}I^{\bullet} &= -k_5^{\bullet}E_1^{\bullet}I^{\bullet} + k_{-5}^{\bullet}C_3^{\bullet},\\
{}_0^{ABC}D_t^{\alpha}C_3^{\bullet} &= k_5^{\bullet}E_1^{\bullet}I^{\bullet} - k_{-5}^{\bullet}C_3^{\bullet} - k_6^{\bullet}C_3^{\bullet},\\
{}_0^{ABC}D_t^{\alpha}P_3^{\bullet} &= k_6^{\bullet}C_3^{\bullet} - k_7^{\bullet}P_3^{\bullet}e_3^{\bullet} + k_{-7}^{\bullet}C_4^{\bullet},\\
{}_0^{ABC}D_t^{\alpha}E_3^{\bullet} &= -k_{-7}^{\bullet}P_3^{\bullet}E_3^{\bullet} + k_{-7}^{\bullet}C_4^{\bullet} + k_8^{\bullet}C_4^{\bullet},\\
{}_0^{ABC}D_t^{\alpha}C_4^{\bullet} &= k_7^{\bullet}P_3^{\bullet}E_3^{\bullet} - k_{-7}^{\bullet}C_4^{\bullet} - k_8^{\bullet}C_4^{\bullet},\\
{}_0^{ABC}D_t^{\alpha}P_4^{\bullet} &= k_8^{\bullet}C_4^{\bullet}.
\end{aligned}
\tag{1}
$$

Table 1 demonstrates the variables used in the model. The model is followed by two reactions, which can be explained by the following mechanism.

1.1. Reaction 1

(1) Binding of methanol $M^{\bullet}$ and alcohol dehydrogenase enzyme (ADH) $E_1^{\bullet}$ takes place in the liver, which results in formaldehyde $P_1^{\bullet}$ and an enzyme-methanol complex $C_1^{\bullet}$. This reaction releases the free alcohol dehydrogenase enzyme (ADH) at the end of this process.

(2) The formaldehyde $P_2^{\bullet}$ starts binding with the formaldehyde dehydrogenase $E_{\bullet}^2$ enzyme at the spot, resulting in the enzyme formaldehyde complex $C_2^{\bullet}$, which then converts into formic acid $P_2^{\bullet}$. This reaction releases $E_2^{\bullet}$.

1.2. Reaction 2

(1) Replacing methanol $M^{\bullet}$, ethanol $I^{\bullet}$ behaves as the substrate and reacts with $E_1^{\bullet}$ to form acetaldehyde $P_3^{\bullet}$. Ethanol complex $C_3^{\bullet}$ is formed as results. This reaction releases the alcohol dehydrogenase enzyme (ADH) $E_1^{\bullet}$.

(2) Acetaldehyde binds with the enzyme acetaldehyde dehydrogenase (ALDH) $E_3^{\bullet}$ and the enzyme acetaldehyde complex $C_4^{\bullet}$ is formed. As a result, acetic acid $P_4^{\bullet}$ is formed and free enzyme $E_3^{\bullet}$ is released.

Table 1: Variables' definitions.

Parameters	Interpretation
$E_1^*(t)$	Alcohol dehydrogenase enzyme
$E_2^*(t)$	Formaldehyde dehydrogenase enzyme
$E_3^*(t)$	Acetaldehyde dehydrogenase enzyme
$M^*(t)$	Methanol
$P_1^*(t)$	Formaldehyde
$P_2^*(t)$	Formic acid
$P_3^*(t)$	Acetaldehyde
$C_1^*, C_2^*, C_3^*, C_4^*(t)$	Substrate-enzyme complexes
$E_4^*(t)$	Free enzyme

Here, $k_1^\bullet, k_2^\bullet, k_3^\bullet, k_4^\bullet, k_5^\bullet, k_6^\bullet, k_7^\bullet$, and $k_8^\bullet$ are the forward rate constants of the problem and $k_{-1}^\bullet, k_{-3}^\bullet, k_{-5}^\bullet$, and $k_{-7}^\bullet$ are the reverse rate constants.

In this work, we will use the drinking model of impulsive differential equations recently published by researchers [25]. Different fractional approaches has been done on drinking; relevant studies on drinking can be seen in [26–28]. To the best of our knowledge, two-scale approach has not been applied to the drinking model along with ABC derivative. So, this work is unique in its nature. The rest of the study is divided in the following sections. At the end of Section 1, basic definitions are provided to be used in coming framework of problem. Section 2 gives an overview of fractional-order drinking model. Section 3 discusses the two-scale transform in detail and subsequent theoretical work. Sections 4 and 5 consist of problem formulation and numerical simulation, respectively. In Section 6, we provide the main results, and we conclude our work in Section 7.

Definition 1. Let σ be a continuous function in (a, b) with $0 < \alpha \le 1$. The fractional-order derivative in ABC sense is defined as [29, 30]

$$ {}_0^{ABC}D_t^\alpha \sigma(t) = \frac{M(\alpha)}{1-\alpha}\frac{\mathrm{d}}{\mathrm{d}t}\int_0^t \sigma(\theta)E_\alpha\left[\frac{-\alpha}{1-\alpha}(t-\theta)^\alpha\right]\mathrm{d}\theta, \quad (2)$$

where $M(\alpha)$ is called normalization constant such that $M(0) = M(1) = 1$.

Definition 2. The fractional integral associated with the fractional derivative can be defined as [29, 30]

$$ {}_0^{ABC}I_t^\alpha \sigma(t) = \frac{1-\alpha}{M(\alpha)}\sigma(t) + \frac{\alpha}{M(\alpha)\Gamma(\alpha)}\int_0^t \left[(t-\theta)^{\alpha-1}\right]\sigma(\theta)\mathrm{d}\theta. \quad (3)$$

2. ABC Fractional-Order Model for Methanol Poisoning

Several researchers and scientists have emphasized fractional calculus in recent decades, demonstrating that fractional calculus better explains natural events than integer order. Fractional calculus has embraced the benefits and popularity of fractal modeling. In this area, we drew inspiration from a fractional mathematical model discussed in a recent research [25]. For the Atangana–Baleanu fractional derivative operator, we adopted a numerical technique. We find the following iterative formula by using the ABC fractional model to (1):

$$\begin{aligned} E_1^\bullet(t) - E_1^\bullet(0) &= \frac{1-\alpha}{M(\alpha)}\left[-k_1^\bullet E_1^\bullet M^\bullet + k_{-1}^\bullet C_1^\bullet + k_2^\bullet C_1^\bullet - k_5^\bullet E_1^\bullet I^\bullet + k_{-5}^\bullet C_3^\bullet + k_6^\bullet C_3^\bullet\right] \\ &+ \frac{\alpha}{M(\alpha)\Gamma(\alpha)}\int_0^t \left[(t-\theta)^{\alpha-1}\right]\left[-k_1^\bullet E_1^\bullet M^\bullet + k_{-1}^\bullet C_1^\bullet + k_2^\bullet C_1^\bullet - k_5^\bullet E_1^\bullet I^\bullet + k_{-5}^\bullet C_3^\bullet + k_6^\bullet C_3^\bullet\right]\mathrm{d}\theta. \end{aligned} \quad (4)$$

To simplify, we take

$$\Omega_1\left(t, E_1^\bullet\right) = -k_1^\bullet E_1^\bullet M^\bullet + k_{-1}^\bullet C_1^\bullet + k_2^\bullet C_1^\bullet - k_5^\bullet E_1^\bullet I^\bullet + k_{-5}^\bullet C_3^\bullet + k_6^\bullet C_3^\bullet. \quad (5)$$

Now, we show that the kernels Ω_i for $i = 1, 2, 3, \ldots, 9$ satisfy the Lipschitz condition and contraction.

3. Two-Scale Transform

There is a famous mathematical conceptual proverb: "If you cannot measure it you cannot manage it." In fact, mathematics is an abstract science of measurements. How about the measurement of a coastline? This example makes the notion of length inapplicable. Length of any coastline is variable and dependent on the scale of measurement. The problem of the coastline is the counterintuitive phenomenon that because the length of the coastline of a landmass is not well described. This stems from the coastlines' fractal curve-like features, i.e., the fact that a coastline usually has a fractal dimension (which literally renders the notion of longitude inapplicable). Benoit Mandelbrot documented the discovery of that phenomenon. The estimated length of the coastline relies on the scheme and the degree of cartographic generalization used to measure it. While there are characteristics of a land mass on all scales, from hundreds of kilometers in size to tiny fractions of one millimeter and below, there is no clear scale of the smallest feature to take into account when measured. The length of a smooth, idealized metal bar can be accurately measured using a measuring instrument to assess that the length is less than a certain amount and greater than

the other. The more accurate the measuring device is, the closer the measurements are to the true value of the metal strip. However, the enhancing measurement instrument does not result in a rise in precision when measuring a coastline. As with the metal pole, for the length of the coastline, there is no way to obtain a definite value; the value simply increases in length. The coastline problem is applied to the idea of fractal surfaces in 3 D space, whereby the area of a surface varies according to the scale of measurement. There are many physical laws that depend on scale and also have scale dependent consequences. In these systems, we can assume that the behavior is "scale" dependent with intense behavioral modifications accompanying the exclusive regimes. After the emergence of Einstein's theory of relativity, scientists believe in relative observation. Implementing the relativity of scale in the same manner, one may conclude the importance of scale dependence in every scientific law. Uncertainty is obvious if the application is taken on the wrong scale. To explain this important fact, two-scale transform is given [31]:

$$\Delta S = \frac{\Delta t^{\alpha}}{\Gamma(1+\alpha)}, \tag{6}$$

where ΔS is the smaller scale and Δt is the larger scale. In existing fractal calculus concepts, two-scale gives reasonable explanation [32]. It is a newly developed idea. It focuses on the importance of scale while analyzing any practical problem. We have been motivated by the researchers. In [33], the presented work became the source of our motivation. We are going to present our work as an example of ideas provided in the mentioned manuscript.

Theorem 1. *The kernel Ω_1 satisfy the Lipchitz condition and contraction if the inequality given below holds*

$$0 \le k_l^{\bullet} l_2 + k_5^{\bullet} l_8 < 1. \tag{7}$$

Proof. Let $a = k_l^{\bullet} l_2 + k_5^{\bullet} l_8$. For $E_1^{\bullet}$, we have

$$\begin{aligned}
\left\|\Omega_1(t, E^{\bullet}) - \Omega_1(t, E_1^{\bullet})\right\| &= -k_1^{\bullet} M^{\bullet}\left(E^{\bullet}(t) - E_1^{\bullet}(t)\right) - k_5^{\bullet} I^{\bullet}\left(E^{\bullet}(t) - E_1^{\bullet}(t)\right) \\
&\le k_1^{\bullet}\left\|M^{\bullet}\right\| \cdot \left\|\left(E^{\bullet}(t) - E_1^{\bullet}(t)\right)\right\| + k_5^{\bullet}\left\|I^{\bullet}\right\| \cdot \left\|\left(E^{\bullet}(t) - E_1^{\bullet}(t)\right)\right\| \\
&= \left(k_1^{\bullet}\left\|M^{\bullet}\right\| + k_5^{\bullet}\left\|I^{\bullet}\right\|\right)\left\|\left(E^{\bullet}(t) - E_1^{\bullet}(t)\right)\right\| \\
&\le \left(k_l^{\bullet} l_2 + k_5^{\bullet} l_8\right)\left\|\left(E^{\bullet}(t) - E_1^{\bullet}(t)\right)\right\|,
\end{aligned} \tag{8}$$

where $\|M^{\bullet}(t)\| \le l_2$ and $\|I^{\bullet}(t)\| \le l_8$ are bounded functions. So, we obtain the following result:

$$\left\|\Omega_1(t, E^{\bullet}) - \Omega_1(t, E_1^{\bullet})\right\| \le a\left\|\left(E^{\bullet}(t) - E_1^{\bullet}(t)\right)\right\|. \tag{9}$$

Thus, for Ω_1, the Lipchitz condition is obtained. Similarly, the Lipschitz condition for Ω_i for $i = 2, 3, 4, \ldots, 13$, also holds. Using this notation, we can write

$$\begin{aligned}
E_1^{\bullet}(t) = E_1^{\bullet}(0) &+ \frac{1-\alpha}{M(\alpha)}\Omega_1(t, E_1^{\bullet}) \\
&+ \frac{\alpha}{M(\alpha)\Gamma(\alpha)}\int_0^t \left[(t-\theta)^{\alpha-1}\right]\Omega_1(t, E_1^{\bullet})\mathrm{d}\theta.
\end{aligned} \tag{10}$$

The recursive formula can be written as

$$\begin{aligned}
E_{1n}^{\bullet}(t) = E_1^{\bullet}(0) &+ \frac{1-\alpha}{M(\alpha)}\Omega_1(t, E_{1n-1}^{\bullet}) \\
&+ \frac{\alpha}{M(\alpha)\Gamma(\alpha)}\int_0^t \left[(t-\theta)^{\alpha-1}\right]\Omega_1(t, E_{1n-1}^{\bullet})\mathrm{d}\theta.
\end{aligned} \tag{11}$$

With initial condition as $E_1^{\bullet}(0) = E_{1_0}^{\bullet}$, the successive terms of difference are defined as follows:

$$\begin{aligned}
\lambda_{1n} = E_{1n}^{\bullet}(t) - E_{1n-1}^{\bullet}(t) = & \\
&\cdot \frac{1-\alpha}{M(\alpha)}\left(\Omega_1(t, E_{1n-1}^{\bullet}) - \Omega_1(t, E_{1n-2}^{\bullet})\right) \\
&+ \frac{\alpha}{M(\alpha)\Gamma(\alpha)}\int_0^t \left[(t-\theta)^{\alpha-1}\right]\left(\Omega_1(t, E_{1n-1}^{\bullet}) - \Omega_1(t, E_{1n-2}^{\bullet})\right)\mathrm{d}\theta.
\end{aligned} \tag{12}$$

Obviously, we obtain

$$E_{1n}^{\bullet}(t) = \sum_{i=0}^{n} \lambda_{1i}(t). \tag{13}$$

We also define

$$E_{1_{-1}}^{\bullet}(0) = 0. \tag{14}$$

Consequently, we obtain the following results:

$$\left\|\lambda_{1n}\right\| \leq \frac{1-\alpha}{M(\alpha)}\gamma_1\left\|\lambda_{1n}\right\| + \frac{\gamma_1\alpha}{M(\alpha)\Gamma(\alpha)}\int_0^t \lambda_{1_{n-1}}(\theta)(t-\theta)^{\alpha-1}\mathrm{d}\theta, \tag{15}$$

where $(\gamma_1, \gamma_2, \gamma_3, \ldots, \gamma_{13}) \in (0,1)^{13}$. By using these results, the existence of the solution is guaranteed. □

Theorem 2. *The model under consideration has a solution if there is a τ_0 such that*

$$\frac{1-\alpha}{M(\alpha)}\gamma_1 + \frac{\tau_0^{\alpha}\gamma_1}{M(\alpha)\Gamma(\alpha)} < 1. \tag{16}$$

Proof. We assume that the model system is consisted of bounded functions. So, we can obtain

$$\left\|\lambda_{1n}\right\| \leq \left\|E_1(0)\right\|\left[\frac{1-\alpha}{M(\alpha)}\gamma_1 + \frac{\tau_0^{\alpha}\gamma_1}{M(\alpha)\Gamma(\alpha)}\right]^n. \tag{17}$$

In order to express (12) as the solution of (1), we suppose that $E_1(t) - E_1(0) = E_n(t) - G_{1_n}(0)$.

Next, we can conclude that

$$\left\|G_{1_n}\right\| \leq \left[\left(\frac{1-\alpha}{M(\alpha)}\right) + \left(\frac{\tau^{\alpha}}{(M(\alpha)\Gamma(\alpha))}\right)\right]^{n-1}\gamma_1^{n-1}, \tag{18}$$

for $\tau = \tau_0$,

$$\left\|G_{1_n}\right\| \leq \left[\frac{1-\alpha}{M(\alpha)} + \frac{\tau_0^{\alpha}}{M(\alpha)\Gamma(\alpha)}\right]^{n-1}\gamma_1^{n-1}. \tag{19}$$

By taking the limit $n \longrightarrow \infty$, we obtain

$$\left\|G_{1_n}(t)\right\| \longrightarrow \infty. \tag{20}$$

With the similar process, we have

$$\left\|G_{i_n}(t)\right\| \longrightarrow \infty, \tag{21}$$

for $i = 1, 2, 3, \ldots, 13$. □

Theorem 3. *model under consideration has a unique solution if*

$$\left[1 - \frac{1-\alpha}{M(\alpha)}\gamma_1 + \frac{\tau^{\alpha}\gamma_1}{M(\alpha)\Gamma(\alpha)}\right] > 0. \tag{22}$$

Proof. First, we assume that the model has another solution, that is, $E_1^{\bullet}$:

$$E_1(t) - E_1^{\bullet}(t) = \frac{1-\alpha}{M(\alpha)}\left(\Omega_1\left(t, E_1 - \Omega_1\left(t, E_1^{\bullet}\right)\right)\right) + \frac{\alpha}{M(\alpha)\Gamma(\alpha)}\int_0^t \left[(t-\theta)^{\alpha-1}\right]\left(\Omega_1\left(t, E_1\right) - \Omega_1\left(t, E_1^{\bullet}\right)\right)\mathrm{d}\theta. \tag{23}$$

By using the properties of norm, we obtain the following inequality:

$$\left\|E_1(t) - E_1^{\bullet}(t)\right\|\left[1 - \frac{1-\alpha}{M(\alpha)}\gamma_1 + \frac{\tau^{\alpha}\gamma_1}{M(\alpha)\Gamma(\alpha)}\right] \leq 0. \tag{24}$$

If condition of (18) is satisfied, then

$$\left\|E_1(t) - E_1^{\bullet}(t)\right\| = 0. \tag{25}$$

Clearly, it is shown that

$$E_1(t) = E_1^{\bullet}(t). \tag{26}$$

Through similar process, we can prove for other components of the model. □

4. Problem Formulation

We suppose the initial-value problem with the ABC fractional derivative:

$${}_0^{ABC}D_{\tau}^{\beta}g(\tau) = f(\tau, g(\tau)). \tag{27}$$

Recently, ABC fractional product integral rule (ABC-PIR) is defined as follows [17]:

$$g_m = g_0 + \frac{\beta h^{\beta}}{M(\beta)}\left(\beta_m f(\tau_0, g_0) + \sum_{i=1}^{n}\zeta_{m-i}f(\tau_i, g_i)\right), \tag{28}$$

where

$$\beta_m = \left(\frac{(m-1)^{\beta+1} - m^{\beta}(m-\beta-1)}{\Gamma(\beta+2)}\right), \tag{29}$$

and ζ_k is

$$\zeta_k = \left(\frac{1}{\Gamma(\beta+2)}\right) + \left(\frac{1-\beta}{\beta h h^{\beta}}\right), \quad \text{for } k = 0,$$

$$\zeta_k = \left(\frac{\left((k-1)^{\beta+1} - 2k^{\beta+1} + (k+1)^{\beta+1}\right)}{\Gamma(\beta+2)}\right), \tag{30}$$

$$\text{for } k = 1, 2, \ldots, m-1.$$

By using (23), our model can be transformed in the following form:

$$E^{\bullet}_{1_n} = E^{\bullet}_0 + \frac{\alpha h^{\alpha}}{M(\alpha)}\left[a_m y_1\left(t_0, M^{\bullet}_0, I^{\bullet}_0, E^{\bullet}_{1_0}, E^{\bullet}_{2_0}, E^{\bullet}_{3_0}, C^{\bullet}_{1_0}, C^{\bullet}_{2_0}, C^{\bullet}_{3_0}, C^{\bullet}_{4_0}, P^{\bullet}_{1_0}, P^{\bullet}_{2_0}, P^{\bullet}_{3_0}, P^{\bullet}_{4_0}\right)\right] + \sum_{i=1}^{m} \zeta_{m-i} y_1\left(t_i, M^{\bullet}_i, I^{\bullet}_i, E^{\bullet}_{1_i}, E^{\bullet}_{2_i}, E^{\bullet}_{3_i}, C^{\bullet}_{1_i}, C^{\bullet}_{2_i}, C^{\bullet}_{3_i}, C^{\bullet}_{4_i}, P^{\bullet}_{1_i}, P^{\bullet}_{2_i}, P^{\bullet}_{3_i}, P^{\bullet}_{4_i}\right). \tag{31}$$

Deriving other equations of model in the same manner, we obtain

$$M^{\bullet}_{1_n} = M^{\bullet}_0 + \frac{\alpha h^{\alpha}}{M(\alpha)}\left[a_m y_2\left(t_0, M^{\bullet}_0, I^{\bullet}_0, E^{\bullet}_{1_0}, E^{\bullet}_{2_0}, E^{\bullet}_{3_0}, C^{\bullet}_{1_0}, C^{\bullet}_{2_0}, C^{\bullet}_{3_0}, C^{\bullet}_{4_0}, P^{\bullet}_{1_0}, P^{\bullet}_{2_0}, P^{\bullet}_{3_0}, P^{\bullet}_{4_0}\right)\right] + \sum_{i=1}^{m} \zeta_{m-i} y_2\left(t_i, M^{\bullet}_i, I^{\bullet}_i, E^{\bullet}_{1_i}, E^{\bullet}_{2_i}, E^{\bullet}_{3_i}, C^{\bullet}_{1_i}, C^{\bullet}_{2_i}, C^{\bullet}_{3_i}, C^{\bullet}_{4_i}, P^{\bullet}_{1_i}, P^{\bullet}_{2_i}, P^{\bullet}_{3_i}, P^{\bullet}_{4_i}\right),$$

$$C^{\bullet}_{1_n} = C^{\bullet}_0 + \frac{\alpha h^{\alpha}}{M(\alpha)}\left[a_m y_3\left(t_0, M^{\bullet}_0, I^{\bullet}_0, E^{\bullet}_{1_0}, E^{\bullet}_{2_0}, E^{\bullet}_{3_0}, C^{\bullet}_{1_0}, C^{\bullet}_{2_0}, C^{\bullet}_{3_0}, C^{\bullet}_{4_0}, P^{\bullet}_{1_0}, P^{\bullet}_{2_0}, P^{\bullet}_{3_0}, P^{\bullet}_{4_0}\right)\right] + \sum_{i=1}^{m} \zeta_{m-i} y_3\left(t_i, M^{\bullet}_i, I^{\bullet}_i, E^{\bullet}_{1_i}, E^{\bullet}_{2_i}, E^{\bullet}_{3_i}, C^{\bullet}_{1_i}, C^{\bullet}_{2_i}, C^{\bullet}_{3_i}, C^{\bullet}_{4_i}, P^{\bullet}_{1_i}, P^{\bullet}_{2_i}, P^{\bullet}_{3_i}, P^{\bullet}_{4_i}\right),$$

$$E^{\bullet}_{2_n} = E^{\bullet}_{2_0} + \frac{\alpha h^{\alpha}}{M(\alpha)}\left[a_m y_5\left(t_0, M^{\bullet}_0, I^{\bullet}_0, E^{\bullet}_{1_0}, E^{\bullet}_{2_0}, E^{\bullet}_{3_0}, C^{\bullet}_{1_0}, C^{\bullet}_{2_0}, C^{\bullet}_{3_0}, C^{\bullet}_{4_0}, P^{\bullet}_{1_0}, P^{\bullet}_{2_0}, P^{\bullet}_{3_0}, P^{\bullet}_{4_0}\right)\right] + \sum_{i=1}^{m} \zeta_{m-i} y_5\left(t_i, M^{\bullet}_i, I^{\bullet}_i, E^{\bullet}_{1_i}, E^{\bullet}_{2_i}, E^{\bullet}_{3_i}, C^{\bullet}_{1_i}, C^{\bullet}_{2_i}, C^{\bullet}_{3_i}, C^{\bullet}_{4_i}, P^{\bullet}_{1_i}, P^{\bullet}_{2_i}, P^{\bullet}_{3_i}, P^{\bullet}_{4_i}\right),$$

$$P^{\bullet}_{1_n} = P^{\bullet}_0 + \frac{\alpha h^{\alpha}}{M(\alpha)}\left[a_m y_4\left(t_0, M^{\bullet}_0, I^{\bullet}_0, E^{\bullet}_{1_0}, E^{\bullet}_{2_0}, E^{\bullet}_{3_0}, C^{\bullet}_{1_0}, C^{\bullet}_{2_0}, C^{\bullet}_{3_0}, C^{\bullet}_{4_0}, P^{\bullet}_{1_0}, P^{\bullet}_{2_0}, P^{\bullet}_{3_0}, P^{\bullet}_{4_0}\right)\right] + \sum_{i=1}^{m} \zeta_{m-i} y_4\left(t_i, M^{\bullet}_i, I^{\bullet}_i, E^{\bullet}_{1_i}, E^{\bullet}_{2_i}, E^{\bullet}_{3_i}, C^{\bullet}_{1_i}, C^{\bullet}_{2_i}, C^{\bullet}_{3_i}, C^{\bullet}_{4_i}, P^{\bullet}_{1_i}, P^{\bullet}_{2_i}, P^{\bullet}_{3_i}, P^{\bullet}_{4_i}\right),$$

$$C^{\bullet}_{2_n} = C^{\bullet}_{2_0} + \frac{\alpha h^{\alpha}}{M(\alpha)}\left[\left(a_m y_6 t_0, M^{\bullet}_0, I^{\bullet}_0, E^{\bullet}_{1_0}, E^{\bullet}_{2_0}, E^{\bullet}_{3_0}, C^{\bullet}_{1_0}, C^{\bullet}_{2_0}, C^{\bullet}_{3_0}, C^{\bullet}_{4_0}, P^{\bullet}_{1_0}, P^{\bullet}_{2_0}, P^{\bullet}_{3_0}, P^{\bullet}_{4_0}\right)\right] + \sum_{i=1}^{m} \zeta_{m-i} y_6\left(t_i, M^{\bullet}_i, I^{\bullet}_i, E^{\bullet}_{1_i}, E^{\bullet}_{2_i}, E^{\bullet}_{3_i}, C^{\bullet}_{1_i}, C^{\bullet}_{2_i}, C^{\bullet}_{3_i}, C^{\bullet}_{4_i}, P^{\bullet}_{1_i}, P^{\bullet}_{2_i}, P^{\bullet}_{3_i}, P^{\bullet}_{4_i}\right),$$

$$P^{\bullet}_{2_n} = P^{\bullet}_{2_0} + \frac{\alpha h^{\alpha}}{M(\alpha)}\left[\left(a_m y_7 t_0, M^{\bullet}_0, I^{\bullet}_0, E^{\bullet}_{1_0}, E^{\bullet}_{2_0}, E^{\bullet}_{3_0}, C^{\bullet}_{1_0}, C^{\bullet}_{2_0}, C^{\bullet}_{3_0}, C^{\bullet}_{4_0}, P^{\bullet}_{1_0}, P^{\bullet}_{2_0}, P^{\bullet}_{3_0}, P^{\bullet}_{4_0}\right)\right] + \sum_{i=1}^{m} \zeta_{m-i} y_7\left(t_i, M^{\bullet}_i, I^{\bullet}_i, E^{\bullet}_{1_i}, E^{\bullet}_{2_i}, E^{\bullet}_{3_i}, C^{\bullet}_{1_i}, C^{\bullet}_{2_i}, C^{\bullet}_{3_i}, C^{\bullet}_{4_i}, P^{\bullet}_{1_i}, P^{\bullet}_{2_i}, P^{\bullet}_{3_i}, P^{\bullet}_{4_i}\right),$$

$$I^{\bullet}_n = I^{\bullet}_0 + \frac{\alpha h^{\alpha}}{M(\alpha)}\left[\left(a_m y_8 t_0, M^{\bullet}_0, I^{\bullet}_0, E^{\bullet}_{1_0}, E^{\bullet}_{2_0}, E^{\bullet}_{3_0}, C^{\bullet}_{1_0}, C^{\bullet}_{2_0}, C^{\bullet}_{3_0}, C^{\bullet}_{4_0}, P^{\bullet}_{1_0}, P^{\bullet}_{2_0}, P^{\bullet}_{3_0}, P^{\bullet}_{4_0}\right)\right] + \sum_{i=1}^{m} \zeta_{m-i} y_8\left(t_i, M^{\bullet}_i, I^{\bullet}_i, E^{\bullet}_{1_i}, E^{\bullet}_{2_i}, E^{\bullet}_{3_i}, C^{\bullet}_{1_i}, C^{\bullet}_{2_i}, C^{\bullet}_{3_i}, C^{\bullet}_{4_i}, P^{\bullet}_{1_i}, P^{\bullet}_{2_i}, P^{\bullet}_{3_i}, P^{\bullet}_{4_i}\right),$$

$$E^{\bullet}_{3_n} = E^{\bullet}_{3_0} + \frac{\alpha h^{\alpha}}{M(\alpha)}\left[a_m y_9\left(t_0, M^{\bullet}_0, I^{\bullet}_0, E^{\bullet}_{1_0}, E^{\bullet}_{2_0}, E^{\bullet}_{3_0}, C^{\bullet}_{1_0}, C^{\bullet}_{2_0}, C^{\bullet}_{3_0}, C^{\bullet}_{4_0}, P^{\bullet}_{1_0}, P^{\bullet}_{2_0}, P^{\bullet}_{3_0}, P^{\bullet}_{4_0}\right)\right] + \sum_{i=1}^{m} \zeta_{m-i} y_9\left(t_i, M^{\bullet}_i, I^{\bullet}_i, E^{\bullet}_{1_i}, E^{\bullet}_{2_i}, E^{\bullet}_{3_i}, C^{\bullet}_{1_i}, C^{\bullet}_{2_i}, C^{\bullet}_{3_i}, C^{\bullet}_{4_i}, P^{\bullet}_{1_i}, P^{\bullet}_{2_i}, P^{\bullet}_{3_i}, P^{\bullet}_{4_i}\right),$$

$$C^{\bullet}_{3_n} = C^{\bullet}_{3_0} + \frac{\alpha h^{\alpha}}{M(\alpha)}\left[a_m y_{10}\left(t_0, M^{\bullet}_0, I^{\bullet}_0, E^{\bullet}_{1_0}, E^{\bullet}_{2_0}, E^{\bullet}_{3_0}, C^{\bullet}_{1_0}, C^{\bullet}_{2_0}, C^{\bullet}_{3_0}, C^{\bullet}_{4_0}, P^{\bullet}_{1_0}, P^{\bullet}_{2_0}, P^{\bullet}_{3_0}, P^{\bullet}_{4_0}\right)\right]$$

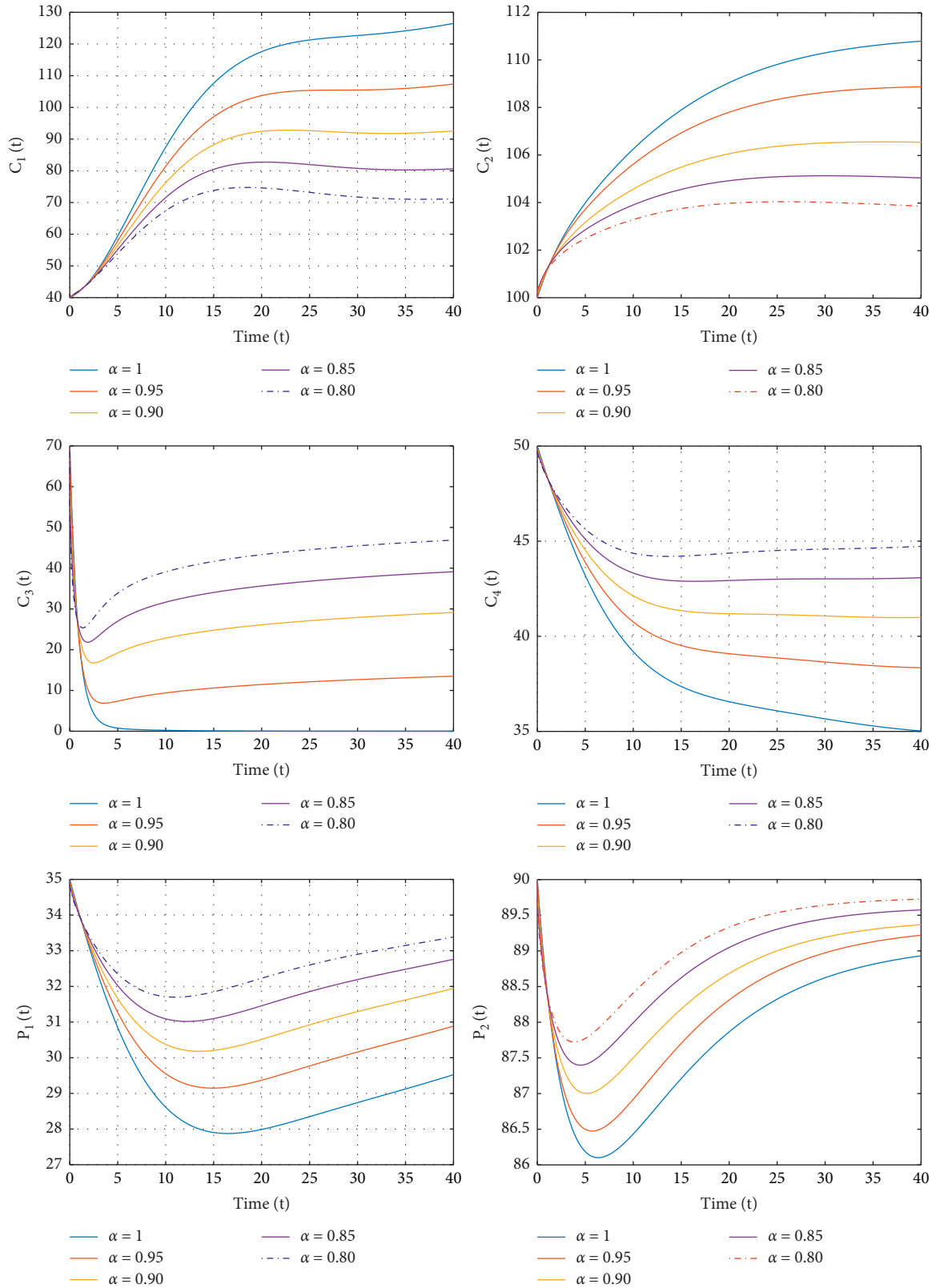

FIGURE 1: Fractional dynamics of reactants C_1, C_2, C_3, C_4, P_1, and P_2 in the enzymatic reaction of drinking model, respectively.

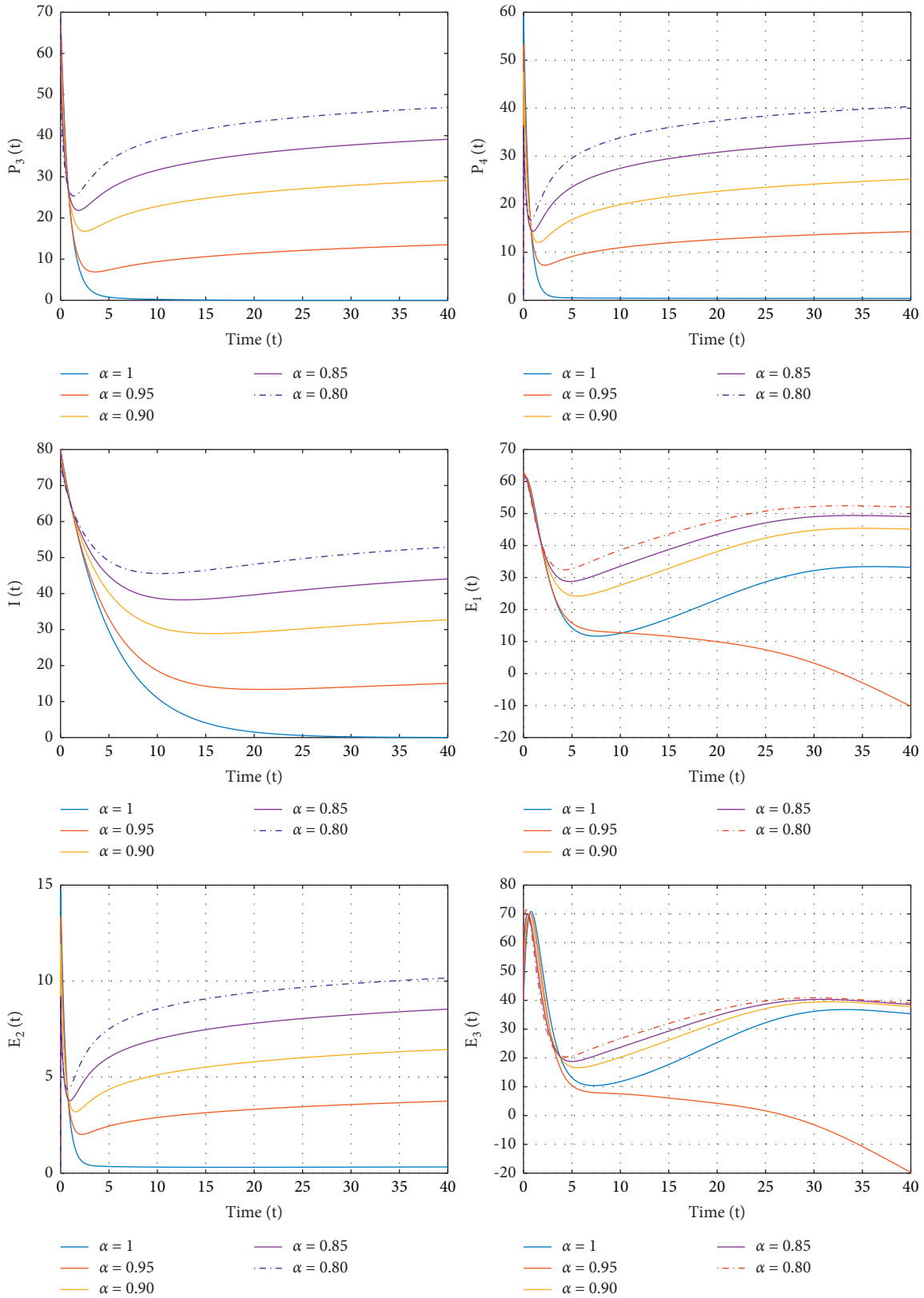

Figure 2: Fractional dynamics of reactants P_3, P_4, I, E_1, E_2, and E_3 in the enzymatic reaction of drinking model, respectively.

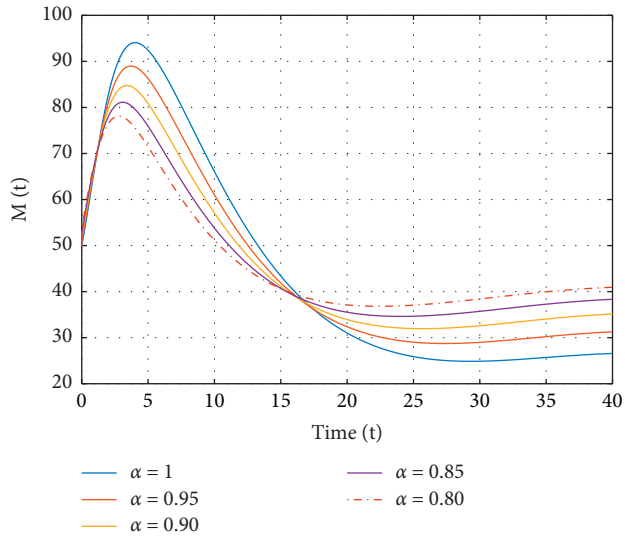

Figure 3: Schematic diagram for reaction process of methanol in the human body.

$$+\sum_{i=1}^{m}\zeta_{m-i}y_{10}\left(t_i,M_i^{\bullet},I_i^{\bullet},E_{1_i}^{\bullet},E_{2_i}^{\bullet},E_{3_i}^{\bullet},C_{1_i}^{\bullet},C_{2_i}^{\bullet},C_{3_i}^{\bullet},C_{4_i}^{\bullet},P_{1_i}^{\bullet},P_{2_i}^{\bullet},P_{3_i}^{\bullet},P_{4_i}^{\bullet}\right),$$

$$P_{3_n}^{\bullet}=P_{3_0}^{\bullet}+\frac{\alpha h^{\alpha}}{M(\alpha)}\left[a_m y_{11}\left(t_0,M_0^{\bullet},I_0^{\bullet},E_{1_0}^{\bullet},E_{2_0}^{\bullet},E_{3_0}^{\bullet},C_{1_0}^{\bullet},C_{2_0}^{\bullet},C_{3_0}^{\bullet},C_{4_0}^{\bullet},P_{1_0}^{\bullet},P_{2_0}^{\bullet},P_{3_0}^{\bullet},P_{4_0}^{\bullet}\right)\right]$$

$$+\sum_{i=1}^{m}\zeta_{m-i}y_{11}\left(t_i,M_i^{\bullet},I_i^{\bullet},E_{1_i}^{\bullet},E_{2_i}^{\bullet},E_{3_i}^{\bullet},C_{1_i}^{\bullet},C_{2_i}^{\bullet},C_{3_i}^{\bullet},C_{4_i}^{\bullet},P_{1_i}^{\bullet},P_{2_i}^{\bullet},P_{3_i}^{\bullet},P_{4_i}^{\bullet}\right),$$

$$C_{4_n}^{\bullet}=C_{4_0}^{\bullet}+\frac{\alpha h^{\alpha}}{M(\alpha)}\left[a_m y_{12}\left(t_0,M_0^{\bullet},I_0^{\bullet},E_{1_0}^{\bullet},E_{2_0}^{\bullet},E_{3_0}^{\bullet},C_{1_0}^{\bullet},C_{2_0}^{\bullet},C_{3_0}^{\bullet},C_{4_0}^{\bullet},P_{1_0}^{\bullet},P_{2_0}^{\bullet},P_{3_0}^{\bullet},P_{4_0}^{\bullet}\right)\right]$$

$$+\sum_{i=1}^{m}\zeta_{m-i}y_{12}\left(t_i,M_i^{\bullet},I_i^{\bullet},E_{1_i}^{\bullet},E_{2_i}^{\bullet},E_{3_i}^{\bullet},C_{1_i}^{\bullet},C_{2_i}^{\bullet},C_{3_i}^{\bullet},C_{4_i}^{\bullet},P_{1_i}^{\bullet},P_{2_i}^{\bullet},P_{3_i}^{\bullet},P_{4_i}^{\bullet}\right),$$

$$P_{4_n}^{\bullet}=P_{4_0}^{\bullet}+\frac{\alpha h^{\alpha}}{M(\alpha)}\left[a_m y_{13}\left(t_0,M_0^{\bullet},I_0^{\bullet},E_{1_0}^{\bullet},E_{2_0}^{\bullet},E_{3_0}^{\bullet},C_{1_0}^{\bullet},C_{2_0}^{\bullet},C_{3_0}^{\bullet},C_{4_0}^{\bullet},P_{1_0}^{\bullet},P_{2_0}^{\bullet},P_{3_0}^{\bullet},P_{4_0}^{\bullet}\right)\right]$$

$$+\sum_{i=1}^{m}\zeta_{m-i}y_{13}\left(t_i,M_i^{\bullet},I_i^{\bullet},E_{1_i}^{\bullet},E_{2_i}^{\bullet},E_{3_i}^{\bullet},C_{1_i}^{\bullet},C_{2_i}^{\bullet},C_{3_i}^{\bullet},C_{4_i}^{\bullet},P_{1_i}^{\bullet},P_{2_i}^{\bullet},P_{3_i}^{\bullet},P_{4_i}^{\bullet}\right). \tag{32}$$

5. Numerical Simulation

We introduce activated charcoal and ethanol to adsorb methanol and suppress the synthesis of hazardous metabolites, based on ABC fractional dynamics of methanol metabolism under the action of the ADH released by the liver.

Dropping • for simplification, we take the $k_1 = 0.1 - 0.3$, $k_{-1} = 0.01 - 0.3, k_2 = 0.2 - 3.5, k_3 = 0.05 - 2.5, k_{-3} = 0.01 - 0.15, k_4 = 0.2 - 2.9, k_5 = 2.5 - 8.0, k_{-5} = 0.2 - 1.85, k_6 = 3.0 - 10.0, k_7 = 1.5 - 5.0, k_{-7} = 0.1 - 1.0, k_8 = 3.5 - 10.0$, $E_{1_0} = 100$, $M_0 = 10, C_{1_0} = 70, P_{1_0} = 60, E_{2_0} = 50, C_{2_0} = 10, P_{2_0} = 30, I_0 = 10, C_{3_0} = 90, P_{3_0} = 80, E_{4_0} = 70, C_{4_0} = 70$, and $P_{4_0} = 100$ for numerical simulation.

Methanol level is lower in patients who get charcoal therapy for the first two hours than in those who do not. As a result, activated charcoal helps preventing toxicity from spreading in the first place.

6. Results and Discussion

From Figures 1 and 2, it is clear that the values of harmful reactants fluctuate when the fractal values for α changes. The value of methanol, which is the model's primary concern, drops rapidly, as shown in Figure 3, and several curves depict the impact of various two-scale dimension on the methanol level in the human body. The lower the fractional parameter is, the less methanol remains in the human body after

activated charcoal is introduced. Because this type of incident is more likely to occur in remote locations, we consider the worst-case scenario, in which travel to the medical center is too long.

Many researchers have employed the ABC fractional operator to represent various illness models, and the findings show that the methodology is accurate. To find a suitable solution, we used the same approach to investigate methanol toxicity, methanol adsorption by activated charcoal, and enzyme-substrate inhibitor dynamics. When activated charcoal is added to the system as soon as possible, the harmful formic acid production slows down. The absorption of methanol by activated charcoal and the enzymatic reaction of methanol in the liver cause methanol concentrations to decline faster. The quick drop in methanol has an impact on the additional reactants in the enzymatic process. Matlab 2020 has been used to get the graphical results. We conclude from these graphical results that, by employing this new concept of the two-sale and ABC fractional operator, one can obtain more accurate results and gain a better knowledge not only of an enzymatic reaction equation system but also of real-world problems in science and engineering.

7. Conclusion

The numerous negative effects of alcohol have been proven. We employed the new ABC fractional derivative to take the alcoholism model into fractional order in this work. The concept of a two-scale fractal dimension has been utilized to elaborate the scale effect in the topic under discussion. Simulations have been used to demonstrate the impact of fractional order. The results demonstrate the effectiveness of the ABC fractional derivative, integral operators, and two-scale transform. Thus, we can claim that the suggested approach is extremely efficient and can be employed to understand the nature of a wide class of nonlinear fractional-order mathematical models in science and engineering.

Data Availability

All the data used to support the findings of the study are available within the article.

Conflicts of Interest

The authors declare that they have no conflicts of interest.

References

[1] W. H. Organization, *Global Status Report on Alcohol and Health 2018*, World Health Organization, Geneva, Switzerland, 2019.

[2] T. Zhao, M. Wang, and Y. Chu, "On the bounds of the perimeter of an ellipse," *Acta Mathematica Scientia*, vol. 42, no. 2, pp. 491–501, 2022.

[3] T.-H. Zhao, M.-K. Wang, G.-J. Hai, and Y.-M. Chu, "Landen inequalities for Gaussian hypergeometric function, revista de la Real academia de Ciencias exactas, físicas y naturales," *Serie A. Matemáticas*, vol. 116, no. 1, pp. 1–23, 2022.

[4] T.-H. Zhao, M.-K. Wang, and Y. Chu, "Concavity and bounds involving generalized elliptic integral of the first kind," *Journal of Mathematical Inequalities*, vol. 15, no. 2, pp. 701–724, 2021.

[5] M. Nadeem and S.-W. Yao, "Solving system of partial differential equations using variational iteration method with He's polynomials," *Journal of Mathematics and Computer Science*, vol. 19, no. 3, pp. 203–211, 2019.

[6] S. N. Hajiseyedazizi, M. E. Samei, J. Alzabut, and Y. M. Chu, "On multi-step methods for singular fractional q-integro-differential equations," *Open Mathematics*, vol. 19, no. 1, pp. 1378–1405, 2021.

[7] H.-Z. Xu, W.-M. Qian, and Y.-M. Chu, "Sharp bounds for the lemniscatic mean by the one-parameter geometric and quadratic means," *Revista de la Real Academia de Ciencias Exactas, Físicas y Naturales. Serie A. Matemáticas*, vol. 116, no. 1, pp. 1–15, 2022.

[8] T.-H. Zhao, B. A. Bhayo, and Y.-M. Chu, "Inequalities for generalized grötzsch ring function," *Computational Methods and Function Theory*, 2021.

[9] M. Nadeem and S.-W. Yao, "Solving the fractional heat-like and wave-like equations with variable coefficients utilizing the Laplace homotopy method," *International Journal of Numerical Methods for Heat & Fluid Flow*, vol. 31, no. 1, pp. 273–292, 2020.

[10] Z.-B. Li and J.-H. He, "Fractional complex transform for fractional differential equations," *Mathematical and Computational Applications*, vol. 15, no. 5, pp. 970–973, 2010.

[11] H.-H. Chu, T.-H. Zhao, and Y.-M. Chu, "Sharp bounds for the toader mean of order 3 in terms of arithmetic, quadratic and contraharmonic means," *Mathematica Slovaca*, vol. 70, no. 5, pp. 1097–1112, 2020.

[12] Y. Chu and T.-H. Zhao, "Concavity of the error function with respect to Hölder means," *Mathematical Inequalities & Applications*, vol. 19, no. 2, pp. 589–595, 2016.

[13] T.-H. Zhao, Z.-H. Shen, and Y.-M. Chu, "Sharp power mean bounds for the lemniscate type means," *Revista de la Real Academia de Ciencias Exactas, Físicas y Naturales. Serie A. Matemáticas*, vol. 115, no. 4, pp. 1–16, 2021.

[14] Y.-Q. Song, T.-H. Zhao, Y.-M. Chu, and X.-H. Zhang, "Optimal evaluation of a toader-type mean by power mean," *Journal of Inequalities and Applications*, vol. 2015, no. 1, pp. 1–12, 2015.

[15] M.-K. Wang, M.-Y. Hong, Y.-F. Xu, Z.-H. Shen, and Y. Chu, "Inequalities for generalized trigonometric and hyperbolic functions with one parameter," *Journal of Mathematical Inequalities*, vol. 14, no. 1, pp. 1–21, 2020.

[16] Y.-M. Chu, U. Nazir, M. Sohail, M. M. Selim, and J.-R. Lee, "Enhancement in thermal energy and solute particles using hybrid nanoparticles by engaging activation energy and chemical reaction over a parabolic surface via finite element approach," *Fractal and Fractional*, vol. 5, no. 3, p. 119, 2021.

[17] S. Rashid, S. Sultana, Y. Karaca, A. Khalid, and Y.-M. Chu, "Some further extensions considering discrete proportional fractional operators," *Fractals*, vol. 30, no. 1, 2022.

[18] T.-H. Zha, O. Castillo, H. Jahanshahi et al., "A fuzzy-based strategy to suppress the novel coronavirus (2019-ncov) massive outbreak," *Applied and Computational Mathematics*, vol. 20, no. 1, pp. 160–176, 2021.

[19] Z.-Y. He, A. Abbes, H. Jahanshahi, N. D. Alotaibi, and Y. Wang, "Fractional-order discrete-time sir epidemic model with vaccination: chaos and complexity," *Mathematics*, vol. 10, no. 2, p. 165, 2022.

[20] F. Jin, Z.-S. Qian, Z.-S. Qian, Y.-M. Chu, and M. U. Rahman, "On nonlinear evolution model for drinking behavior under caputo-fabrizio derivative," *Journal of Applied Analysis & Computation*, vol. 12, no. 2, pp. 790–806, 2022.

[21] M. Nazeer, F. Hussain, M. I. Khan et al., "Theoretical study of mhd electro-osmotically flow of third-grade fluid in micro channel," *Applied Mathematics and Computation*, vol. 420, Article ID 126868, 2022.

[22] Y.-M. Chu, B. M. Shankaralingappa, B. J. Gireesha, F. Alzahrani, M. I. Khan, and S. U. Khan, "Combined impact of cattaneo-christov double diffusion and radiative heat flux on bio-convective flow of Maxwell liquid configured by a stretched nano-material surface," *Applied Mathematics and Computation*, vol. 419, Article ID 126883, 2022.

[23] T. H. Zhao, M. I. Khan, and Y. M. Chu, "Artificial neural networking (ANN) analysis for heat and entropy generation in flow of non-Newtonian fluid between two rotating disks," *Mathematical Methods in the Applied Sciences*, 2021.

[24] M. A. Iqbal, Y. Wang, M. M. Miah, and M. S. Osman, "Study on Date-Jimbo-Kashiwara-Miwa Equation with Conformable Derivative Dependent on Time Parameter to Find the Exact Dynamic Wave Solutions," *Fractal and Fractional*, vol. 6, no. 1, p. 4, 2021.

[25] P. Ghosh and J. F. Peters, "Impulsive differential equation model in methanol poisoning detoxification," *Journal of Mathematical Chemistry*, vol. 58, no. 1, pp. 126–145, 2020.

[26] S. Lee, E. Jung, and C. Castillo-Chavez, "Optimal control intervention strategies in low- and high-risk problem drinking populations," *Socio-Economic Planning Sciences*, vol. 44, pp. 258–265, 2010.

[27] H. F. Huo, Y. L. Chen, and H. Xiang, "Stability of a binge drinking model with delay," *Journal of biological dynamics*, vol. 11, pp. 210–225, 2017.

[28] Q. T. Ain, N. Anjum, A. Din, A. Zeb, S. Djilali, and Z. A. Khan, "On the analysis of Caputo fractional order dynamics of middle east lungs coronavirus (MERS-CoV) model," *Alexandria Engineering Journal*, vol. 61, no. 7, pp. 5123–5131, 2022.

[29] A. Atangana, "Fractal-fractional differentiation and integration: Connecting fractal calculus and fractional calculus to predict complex system," *Chaos, Solitons & Fractals*, vol. 102, pp. 396–406, 2017.

[30] A. Atangana and S. Qureshi, "Modeling attractors of chaotic dynamical systems with fractal-fractional operators," *Chaos, Solitons & Fractals*, vol. 123, pp. 320–337, 2019.

[31] Q. T. Ain and J.-H. He, "On two-scale dimension and its applications," *Thermal Science*, vol. 23, no. 3, pp. 1707–1712, 2019.

[32] J.-H. He and Q.-T. Ain, "New promises and future challenges of fractal calculus: from two-scale thermodynamics to fractal variational principle," *Thermal Science*, vol. 24, no. 2, pp. 659–681, 2020.

[33] J.-H. He, G. M. Moatimid, and M. H. Zekry, "Forced Nonlinear Oscillator in a Fractal Space," *Facta Universitatis, Series: Mechanical Engineering 20*, no. 1, p. 1, 2022.